HSR Airframe Technical Review
Configuration Aerodynamics

Model 2b Test Results

Aga M. Goodsell
NASA Ames Research Center
February 11, 1998

Viewgraph 1: Session 5: Configuration Assessments and Fundamental Studies

This activity is part of the Wind Tunnel Database and Wind Tunnel Data Corrections Programs. The main purpose of this test was to evaluate the aerodynamic performance of the TCA Baseline configuration around the supersonic cruise point.

Session 5: Configuration Assessments and Fundamental Studies

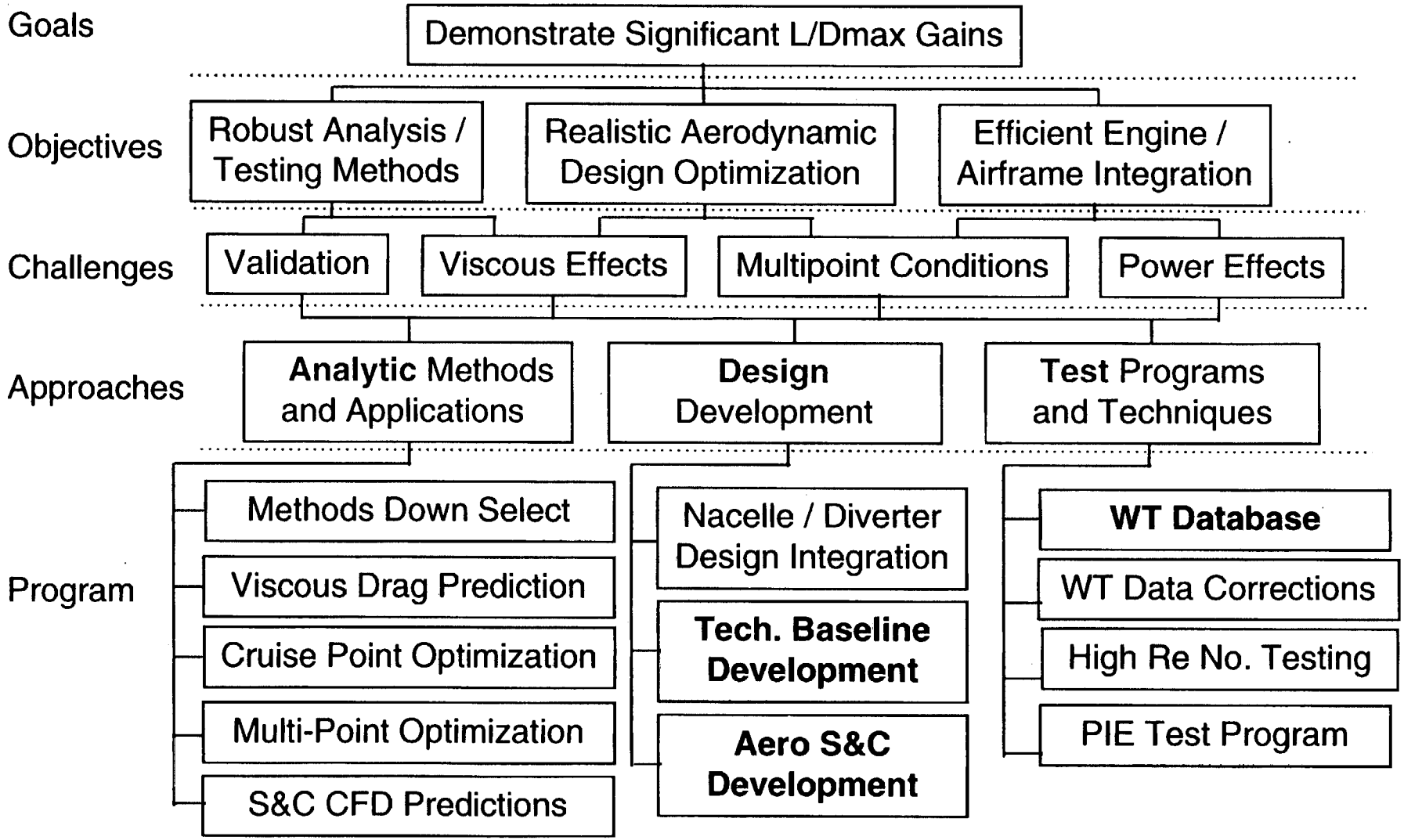

Viewgraph 2: Test 1679 Summary

This test was conducted at NASA Langley Research Center in Test Section #2 of the Unitary Pressure Wind Tunnel. The test was conducted over a period of five weeks between January 21 and February 25, 1997. Both of the 1.675%-scale TCA Baseline models—Model 2a and Model 2b—were tested. There are two main differences between the models. Model 2a has cutouts for leading and trailing edge flaps and is instrumented with both upper and lower surface pressure taps. On the other hand, Model 2b was built with a solid wing with only two pressure tubes installed to measure nacelle base pressures.

Test 1679 Summary

- Test conducted at LaRC UPWT #2
- Test dates: 1/21/97–2/25/97
- 1.675% Baseline TCA Models tested
  - Model 2a with modular wing
  - Model 2b with solid wing

Viewgraph 3: Test 1679 Objectives

The main objective of test 1679 was to establish Model 2b as a calibration model for future HSR performance tests. Therefore, it was important to obtain high quality performance data at the cruise Mach number of 2.4. As part of this requirement, the goal was to achieve an uncertainty in the measured drag coefficient equal to ±0.5 counts at 80% confidence. In addition, a comparison of the performance data was made between Models 2a and 2b to evaluate the effects of leading- and trailing-edge flaps and cutouts for pressure tubing on the data.

The second objective of the test was to try to assess the drag due to the trip dots that were applied to the configurations to attain transition from laminar to turbulent flow. To attempt to meet this objective, the dot heights were varied and the resulting aerodynamic forces were measured. Then, sublimation photographs were obtained to observe the resulting transition location in order to determine if the trip dots were effective at tripping the flow.

Test 1679 Objectives

- Establish Model 2b as a calibration model
  - Obtain high quality performance data at M_∞=2.4 ($\Delta C_D = \pm 0.5$ cts @ 80% confidence)
  - Compare performance between Models 2a & 2b
- Assess trip drag of Model 2b WB & WBND
  - Measure forces w/ varying trip dot height
  - Obtain sublimation photos; determine transition location

Viewgraph 4: Model 2b upper surface

This is a photograph of the upper surface of Model 2b in the test section. The wing/body configuration consists of three main pieces of hardware: the nose assembly, the wing/strongback with an upper balance cover, and the truncated aft fuselage. All sharp leading and trailing edges were modified to accommodate 0.004 inch thicknesses.

Model 2b Upper Surface

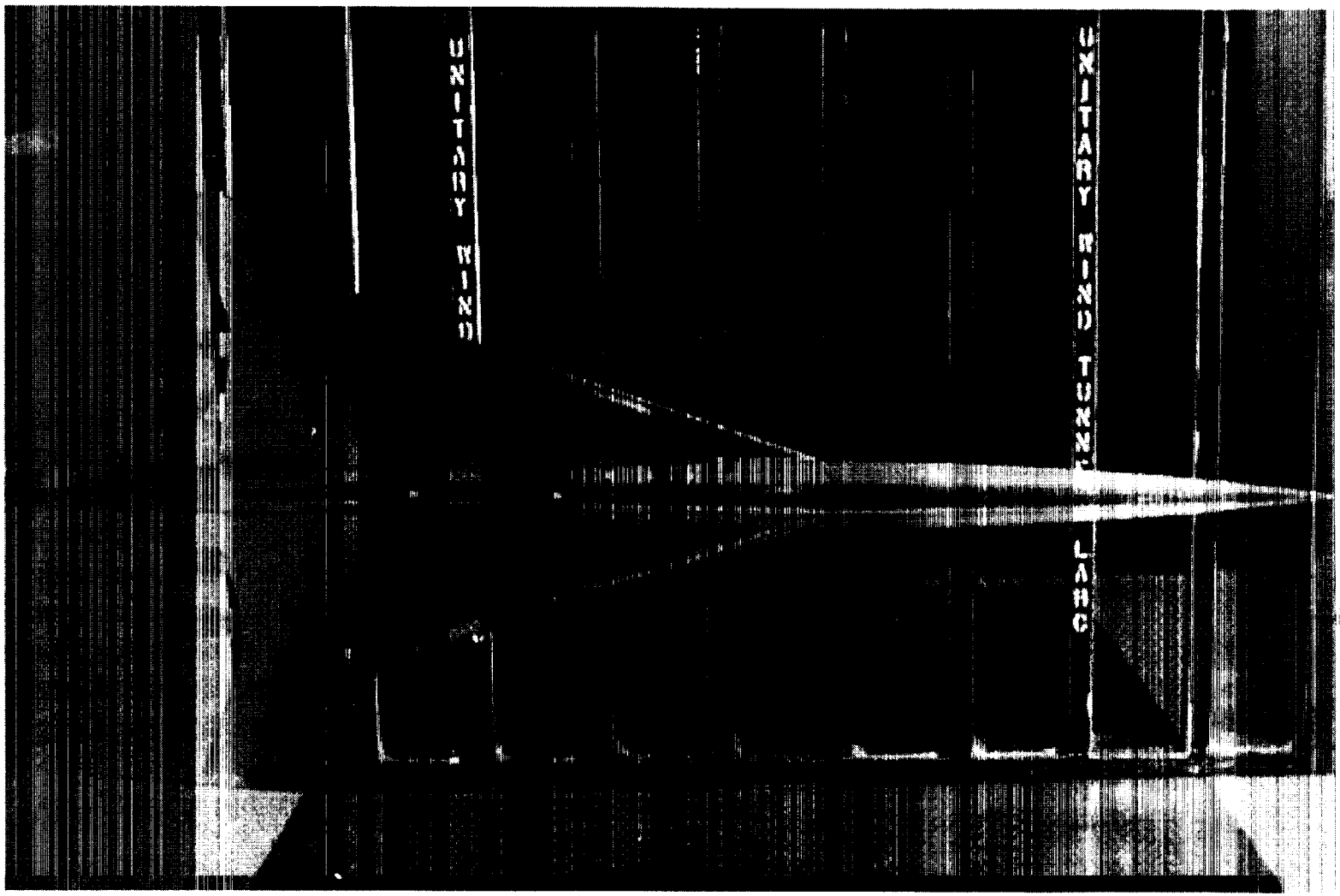

Viewgraph 5: Model 2b lower surface

This photograph shows the lower surface of the model including the nacelles. The diverters were built as an integral part of the nacelles. The lip thicknesses of the nacelles were less than 0.004 inch and the sidewalls of the exit were approximately 0.004 inch thick. The internal duct of the nacelles were fabricated using a wire EDM to save manufacturing time and costs. Therefore, the internal duct was constructed as a linear loft between the circular inlet and the square exit. As a result, the internal duct is different from the OML definition. However, the area of the internal duct varies by less than 0.1%. The two left-hand nacelles were instrumented with four base pressure taps—two on the upper base area and two on the lower base area. The four taps were manifolded into one tube so that an average base pressure was measured during testing.

Model 2b Lower Surface

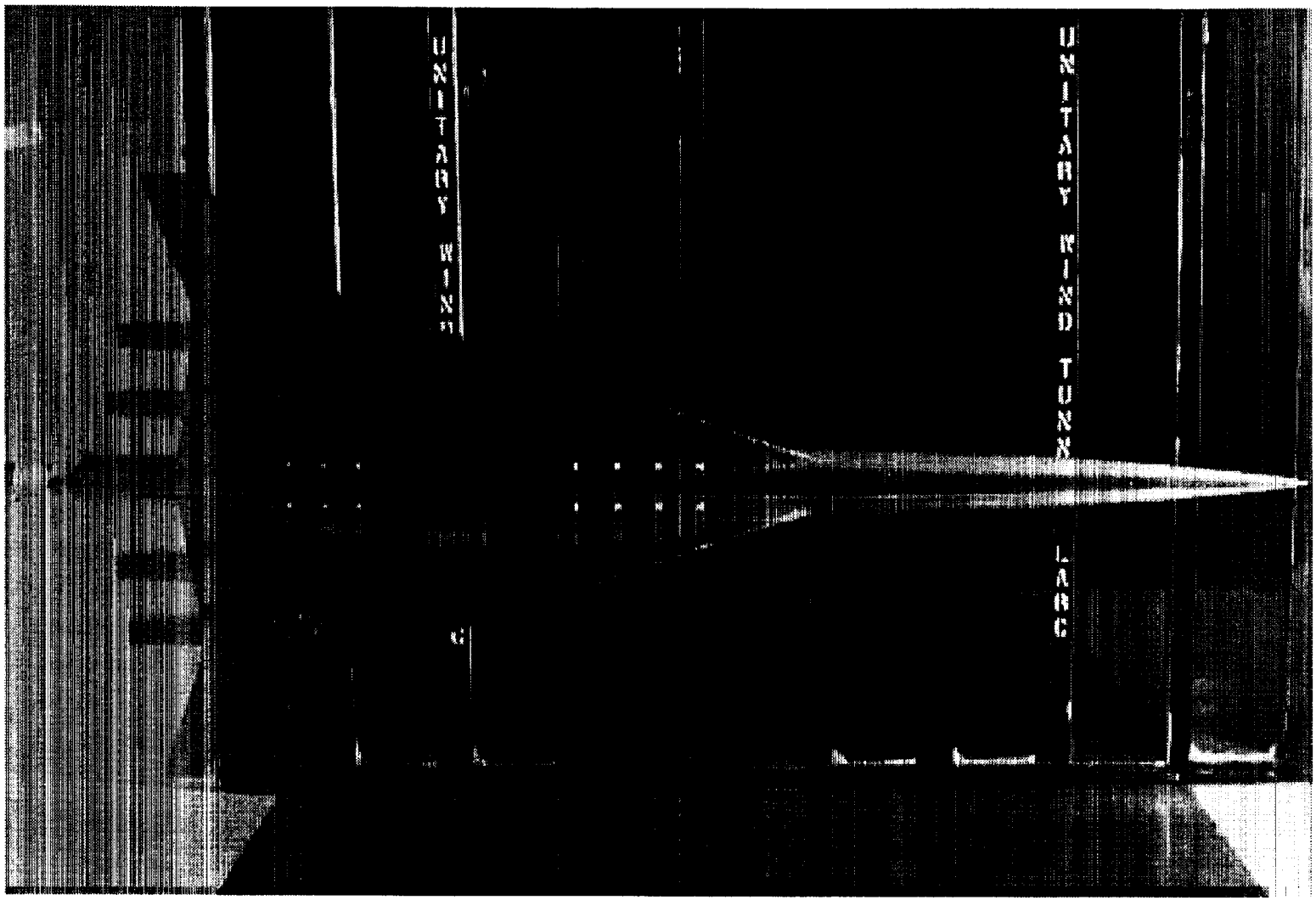

Viewgraph 6: Data Acquired

Forces and moments were first obtained on Model 2a at freestream Mach 2.4 and 2.7 at two Reynolds numbers—4×10^6/ft and 3×10^6/ft. Since an earlier test entry at UPWT (Test 1671) involved an extensive study on Model 2a, another thorough study of Model 2a was not necessary. Therefore, Model 2a was tested first to make sure that the tunnel was operating consistently, since previous data was available to compare with the current data, and to obtain data for a long-term repeatability analysis. Next, Model 2b was installed in the tunnel. Then, forces and moments were obtained at the same conditions as that of Model 2a. In addition to forces and moments, two flow visualization procedures were conducted. Colored oil flow photographs were acquired at two angles-of-attack—0° and 3.5°—at supersonic cruise Mach 2.4. As mentioned previously, sublimation photographs were also taken for the different trip configurations at the cruise point.

Data Acquired

- Model 2a (WB and WBNDf)
  - Forces, Moments
    - M_∞=2.4, 2.7, Re=4x10^6/ft, 3x10^6/ft
- Model 2b (WB and WBNDf)
  - Forces, Moments
    - M_∞=2.4, 2.7, Re=4x10^6/ft, 3x10^6/ft
  - Colored oil flow
    - M_∞=2.4 at $\alpha = 0^\circ, 3.5^\circ$
  - Sublimation
    - M_∞=2.4 at $\alpha = 3.5^\circ$ (cruise only)

Viewgraph 7: Drag Data Reduction

In the final data reduction of the forces, several corrections are made to the drag coefficient involving the internal drag of the nacelles, the base pressure acting on the nacelles, and the fuselage cavity pressure.

The internal drag of the nacelles is computed using skin friction coefficients, based on the inlet Mach number from CFD calculations, obtained from Boeing Long Beach "Clutter" charts. These skin friction coefficients are calculated from flat plate theory and corrected for compressibility effects. The skin friction coefficient is applied to the wetted area of the internal duct to obtain the internal drag. This internal drag estimate is then subtracted from the measured drag.

An average base pressure is measured on one inboard nacelle and one outboard nacelle during testing. The base pressure drag due to each nacelle is computed by assuming that the average base pressure acts on the entire base area of the nacelle and is also subtracted from the measured drag.

Finally, two pressure tubes are attached to the sting and are used to measure the cavity pressure inside the aft fuselage. This pressure is applied to the base cavity area and is subtracted from the measured drag.

Drag Data Reduction

- Nacelle Internal Drag Correction
  - Skin friction coefficient obtained from BLB "Clutter" charts using inlet Mach number
- Nacelle Base Pressure Correction
  - Base pressure measured during testing
- Fuselage Cavity Pressure Correction
  - Cavity pressure measured during testing

Viewgraph 8: Drag Polars @ M_∞=2.4

The figure on the left gives the drag polar near C_{Dmin} and the figure on the right gives the drag polar near cruise. The lift and drag for both the wing/body (W/B) and the wing/body/nacelle/diverter/ fairing (WBNDf) configurations are included in the figures. The drag polars show that Model 2b has less drag than model 2a for both configurations at the two flight conditions.

Drag Polars @ M_∞=2.4

SYMBOL	CONFIGURATION	RUN
—o—	TCA Model 2a WB	3
—o—	TCA Model 2a WB	5
—o—	TCA Model 2a WB	6
·····o·····	TCA Model 2a WBNDf	9
·····o·····	TCA Model 2a WBNDf	11
·····o·····	TCA Model 2a WBNDf	12
—□—	TCA Model 2b WB	16
—□—	TCA Model 2b WB	18

SYMBOL	CONFIGURATION	RUN
—□—	TCA Model 2b WB	19
—□—	TCA Model 2b WB	20
—□—	TCA Model 2b WB	21
—□—	TCA Model 2b WB	22
·····□·····	TCA Model 2b WBNDf	29
·····□·····	TCA Model 2b WBNDf	31
·····□·····	TCA Model 2b WBNDf	32

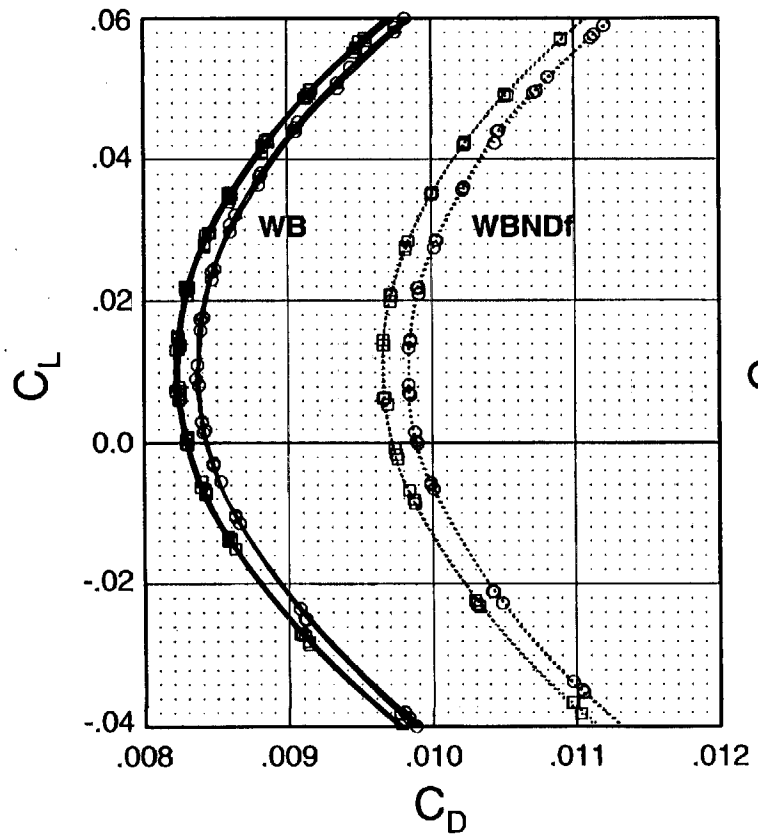

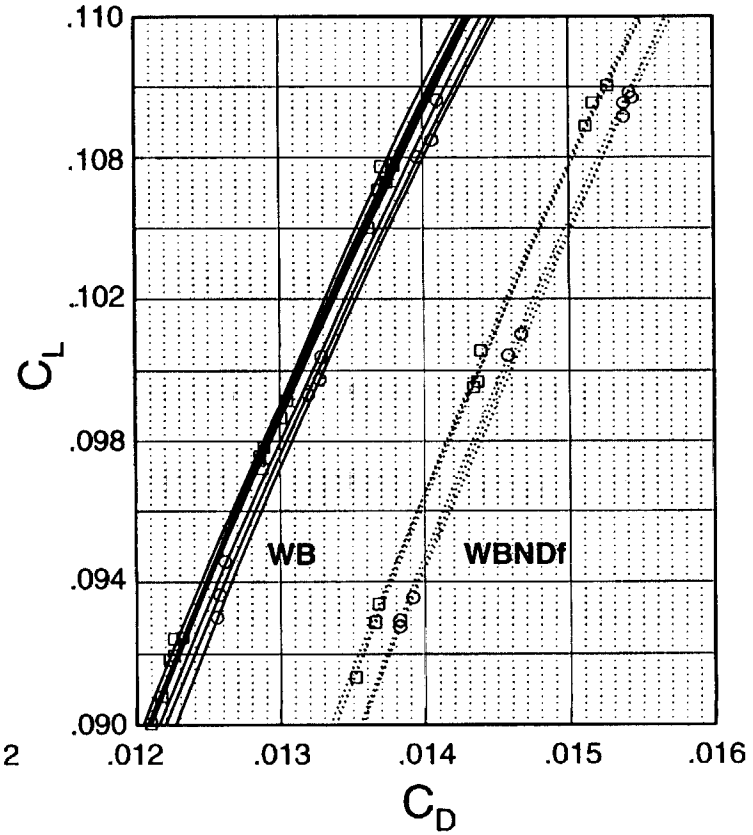

Viewgraph 9: Model 2a/2b Comparison

This chart summarizes the differences in drag between the two wind tunnel models. At cruise conditions, Model 2b produces approximately 1.5 counts less drag than Model 2a for the WB configuration. The WBNDf configuration of Model 2b has about 2.0 counts less drag than that of Model 2a at cruise. The drag increment between the two models is different for the WB and WBNDf configurations because of the differences in the drag increment due to the nacelles. The nacelle increment of Model 2a is slightly greater than that of Model 2b at both C_{Dmin} and cruise as shown in the following chart. This may be a result of manufacturing differences between the two sets of nacelles.

Model 2a/2b Comparison

- WB $\Delta C_{Dcruise} = 1.5$ cts
- WBNDf $\Delta C_{Dcruise} = 2.0$ cts
- Model 2a Nacelle Increment
  - @ C_{Dmin} $\Delta C_D = 14.5$ cts
  - @ $C_{Dcruise}$ $\Delta C_D = 12.8$ cts
- Model 2b Nacelle Increment
  - @ C_{Dmin} $\Delta C_D = 14.0$ cts
  - @ $C_{Dcruise}$ $\Delta C_D = 12.5$ cts

Viewgraph 10: Colored Oil Flow

This photograph shows the colored oil flow on the upper surface of Model 2b at freestream Mach 2.4 and 3.5° angle-of-attack. The oil flow shows that the flow is attached and that there is only a slight amount of crossflow on the upper surface.

Colored Oil Flow

$M_\infty = 2.4$, $\alpha = 3.5^\circ$, Upper Surface

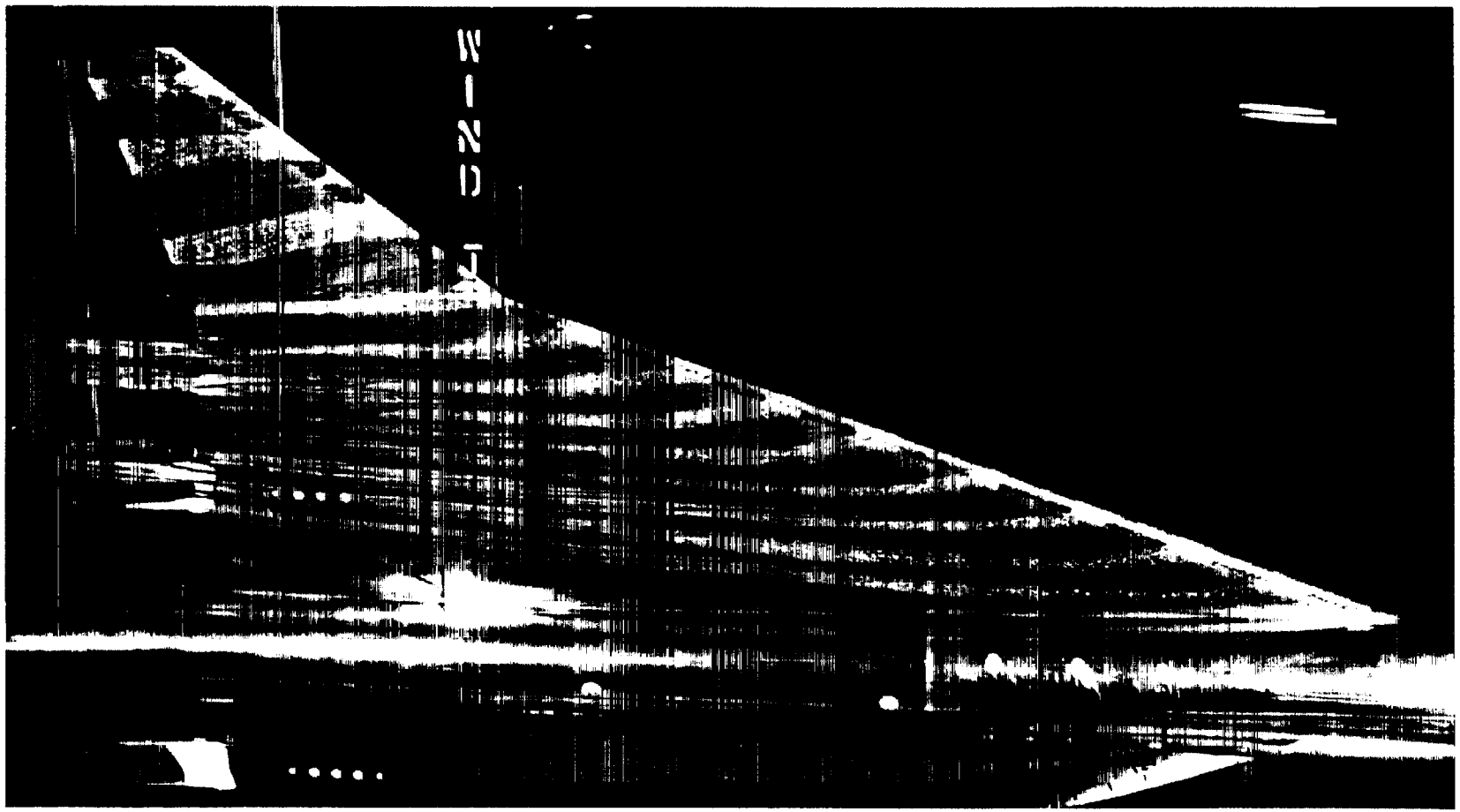

Viewgraph 11: Colored Oil Flow

This photograph shows the colored oil flow on the lower surface of Model 2b at freestream Mach 2.4 and 3.5° angle-of-attack near the nacelles. The oil flow shows that the flow is streamwise over the entire lower surface, except near the nacelles. In this region, the effects of the shock waves from the nacelle inlets on the lower surface flowfield are visible.

Colored Oil Flow

$M_\infty = 2.4$, $\alpha = 3.5^\circ$, Lower Surface

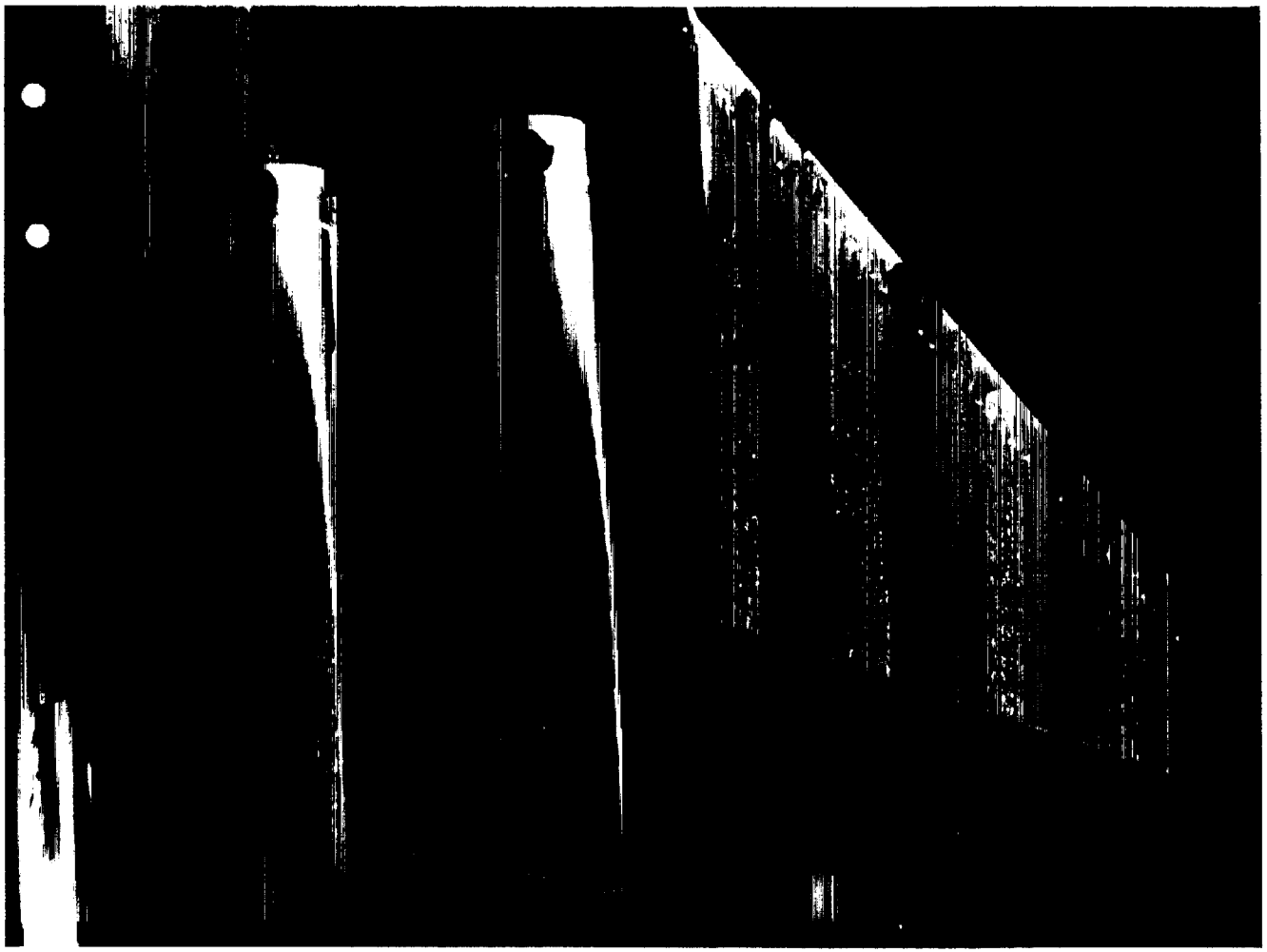

Viewgraph 12: Trip Drag Study

A trip drag study was conducted by varying the trip dot height on the wing surfaces and the nacelles. The trip dots on the nose remained fixed at a streamwise location of 1.0 inch and were 0.012 inch in height. All of the trip dots on the wing and nacelles were applied at a streamwise location equal to 0.6 inch downstream of the leading edges.

The first part of the study was conducted on the WB configuration and involved changing the trip dots on the entire wing. The following trip dot heights were tested: 0.006", 0.008", 0.010", 0.012", 0.014", 0.017". Sublimation photographs were obtained on both upper and lower surfaces for all configurations.

The second part of the study was again conducted on the WB configuration and involved changing the trip dots on the inboard upper surface only. The same trip dot heights between 0.006" and 0.014" that were used on the entire wing were also used on the inboard upper surface. The remaining wing surfaces were maintained at 0.012". Sublimation photographs were not obtained for these configurations.

Trip Drag Study

- Nose Trip Dot Height 0.012″ at x = 1.0″
- WB & Nacelle trip dots at x = 0.6″
- WB Entire Wing Trip Heights:
  - 0.006″, 0.008″, 0.010″, 0.012″, 0.014″, 0.017″
  - Sublimation obtained on all configurations
- WB Inboard Upper Wing Trip Heights:
  - 0.006″, 0.008″, 0.010″, 0.012″, 0.014″
  - Remaining wing at 0.012″

Viewgraph 13: Trip Drag Study, continued

The third part of the study used the WBNDf configuration and involved changing the trip dots on the nacelles only. The trip dots on the entire wing were maintained at 0.012". Three trip configurations were used on the nacelles—0.008", 0.012", and 0.014". Sublimation photographs were obtained on the upper and lower surfaces of the wing including the nacelles.

Various other trip configurations were also tested on the WB configuration. All trip configurations were removed from the wing in order to obtain data for free transition. In addition, 0.0127" glass beads and 0.0117" grit were each applied to the entire wing and tested to observe differences in the transition location. Finally, 0.010" trip dots applied at 0.4 inch downstream of the leading edges on the wing were tested. Sublimation photographs were obtained on all of the alternate trip configurations including free transition.

Trip Drag Study

- WBNDf Nacelle Trip Heights:
  - 0.008″, 0.012″, 0.014″
  - WB trip height 0.012″
- WB Other Trip Configurations:
  - Free Transition
  - 0.0127″ Glass Beads at x=0.6″
  - 0.0117″ Grit at x=0.6″
  - 0.010″ Trip Dots at x=0.4″

Viewgraph 14: Drag vs Trip Height @ C_{Dmin}

This plot shows the variation in the drag of the WB and WBNDf configurations as a function of the trip dot height at C_{Dmin}. The drag of the WB configuration at the free transition condition is also included in the plot. The variation in the drag of the WB configuration which has the same trip configuration applied to the entire wing is linear between trip dot heights equal to 0.006" and 0.012" and between 0.012" and 0.017", but with two different slopes. In addition, the drag of the WB configuration varies nearly linearly over the range of trip dot heights when only the inboard upper wing trip configuration is changed. For the WBNDf configuration, the drag also varies linearly with changes to the trip dot height on the nacelles.

Drag vs Trip Height @ $C_{D_{min}}$

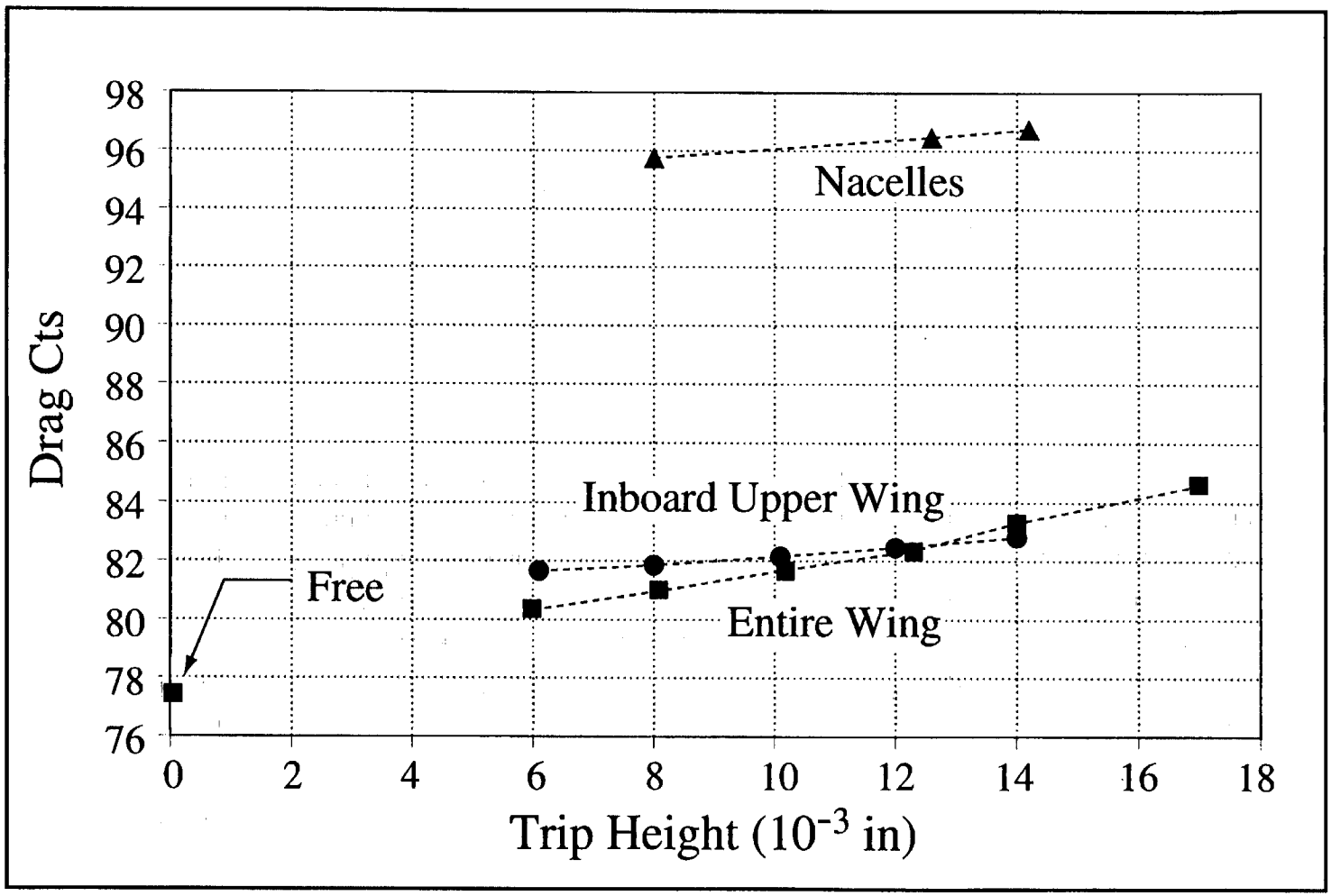

Viewgraph 15: Drag vs Trip Height @ cruise

This plot shows the variation in the drag of the WB and WBNDf configurations as a function of the trip dot height at the cruise condition. Once again, the drag of the WB configuration at the free transition condition is also included in the plot. At cruise, the variation in drag of the WB configuration which has the same trip dot height over the entire wing is no longer linear. In addition, the drag of the WBNDf configuration does not vary linearly with a change in the trip dot configuration of the nacelles. However, the drag of the WB configuration appears to vary linearly when the trip dots are changed only on the inboard upper surface.

Drag vs Trip Height @ Cruise

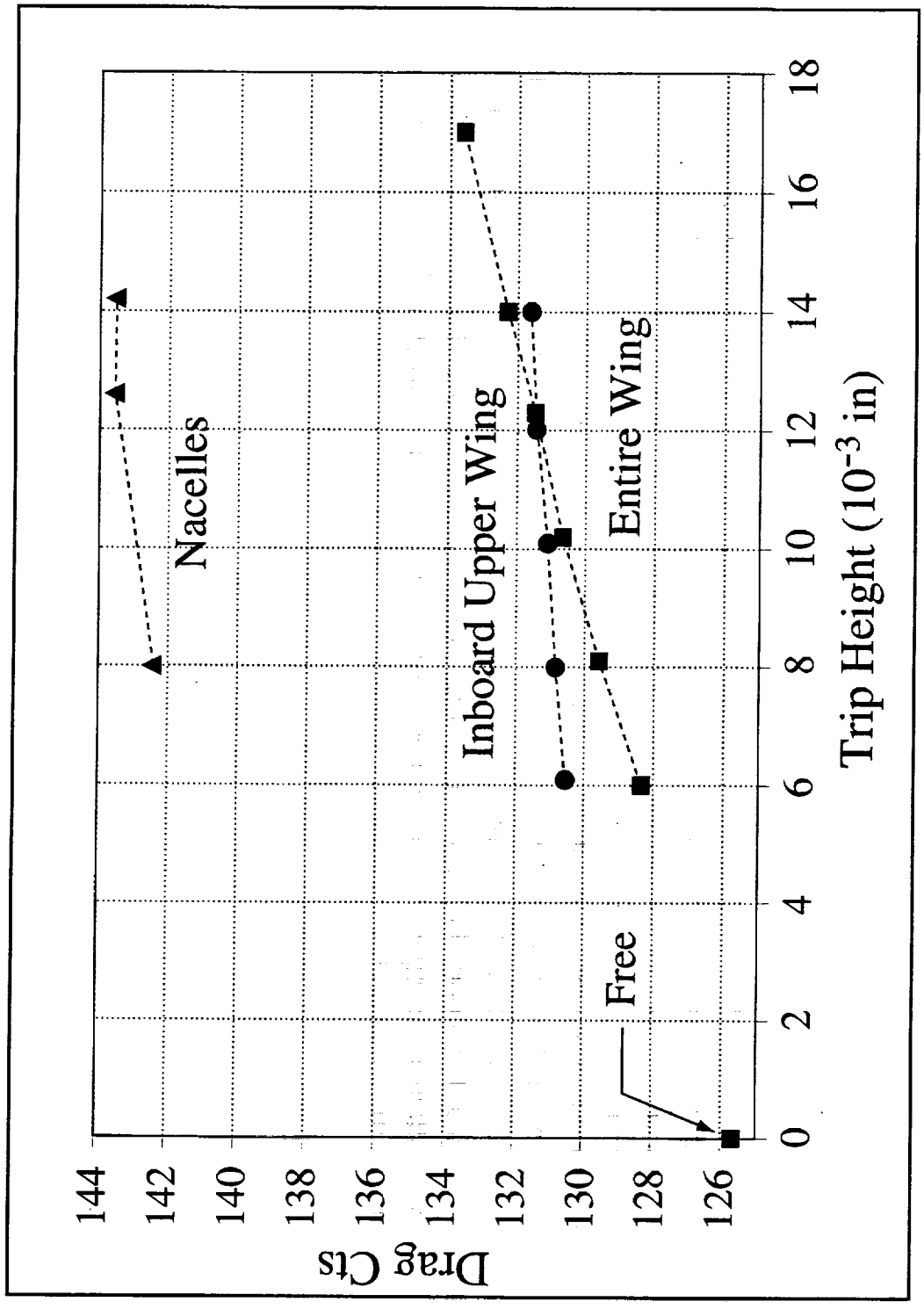

Viewgraph 16: Sublimation Process

The sublimation material that was sprayed onto the upper and lower surfaces of the model consisted of a saturated solution of fluorene in ethanol, which was run through a course filter. The model was installed in a vertical position for the flow visualization runs in order to allow photographs to be taken during the runs. Two cameras were installed, one on each side of the test section, to capture the photographs during the sublimation process. Installation of the cameras to allow optimum visual access was impeded as a result of the steel webs that were part of the windows on each side of the test section. This also made the lighting more difficult to control which resulted in some glare on the bare spots of the model that appeared during sublimation. Once the Mach number and angle-of-attack were attained during each run, pictures were taken every 30 seconds until the majority of the fluorene had sublimed on both surfaces.

Sublimation Process

- Saturated solution of fluorene in ethanol (run through a coarse filter)
- Camera installed on each side of test section
  - Visual access impeded by webs on windows
  - Lighting difficult to control, resulting in glare
- Pictures taken every 30 sec until majority of fluorene had sublimed

Viewgraph 17: Sublimation Photo, Free Transition, Upper Surface

This photograph clearly shows the location of natural transition on the upper surface. Near the wing/body intersection, transition occurs close to the leading edge. The transition location moves further downstream of the leading edge away from the wing/body intersection. The majority of the flow in the outboard region remains laminar.

Sublimation Photo

Free Transition, Upper Surface

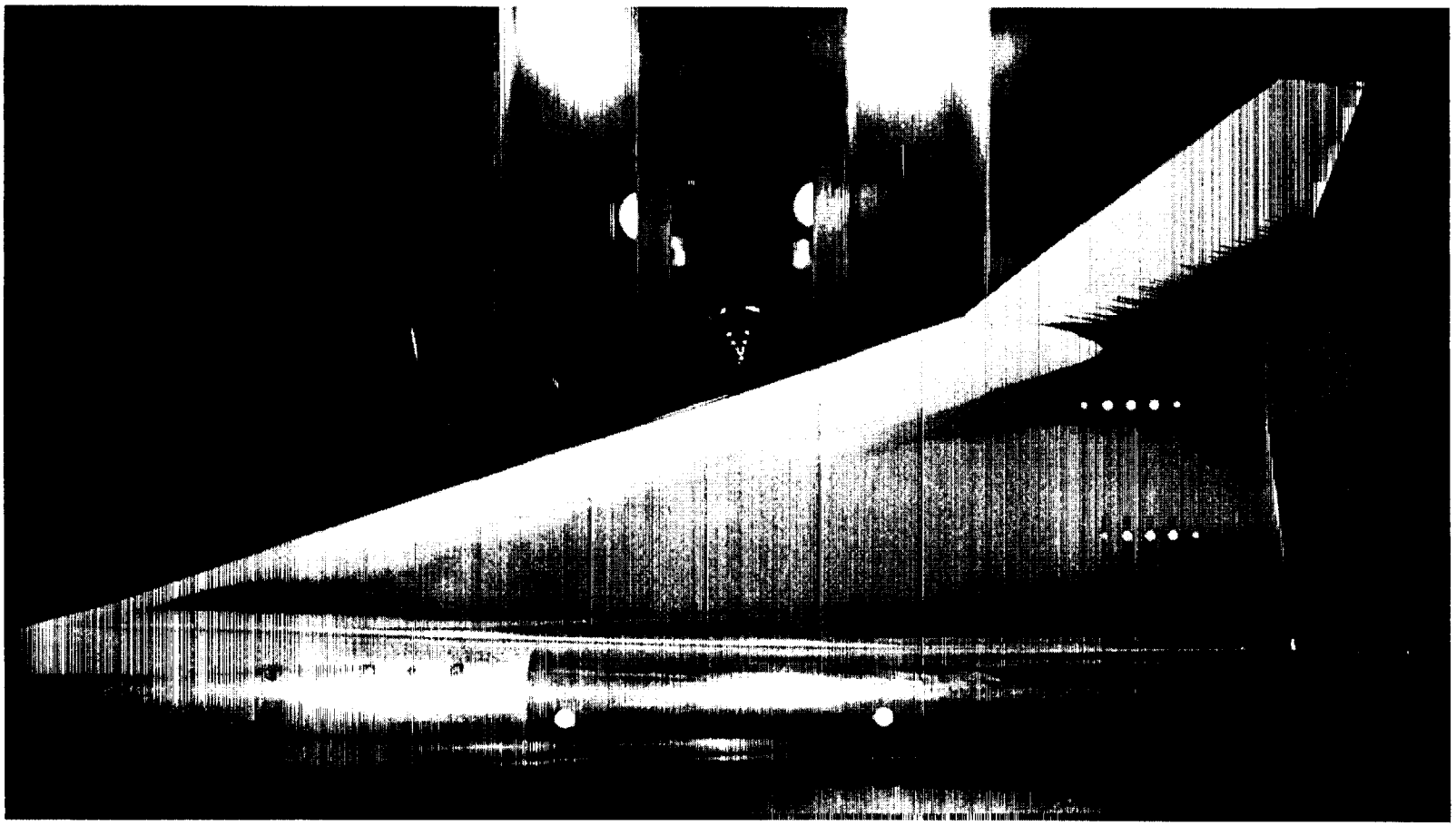

Viewgraph 18: Sublimation Photo, Free Transition, Lower Surface

On the lower surface, natural transition occurs closer to the leading edge than on the upper surface in both the inboard and outboard regions. Nevertheless, the outboard region still maintains a large portion of laminar flow.

Sublimation Photo

Free Transition, Lower Surface

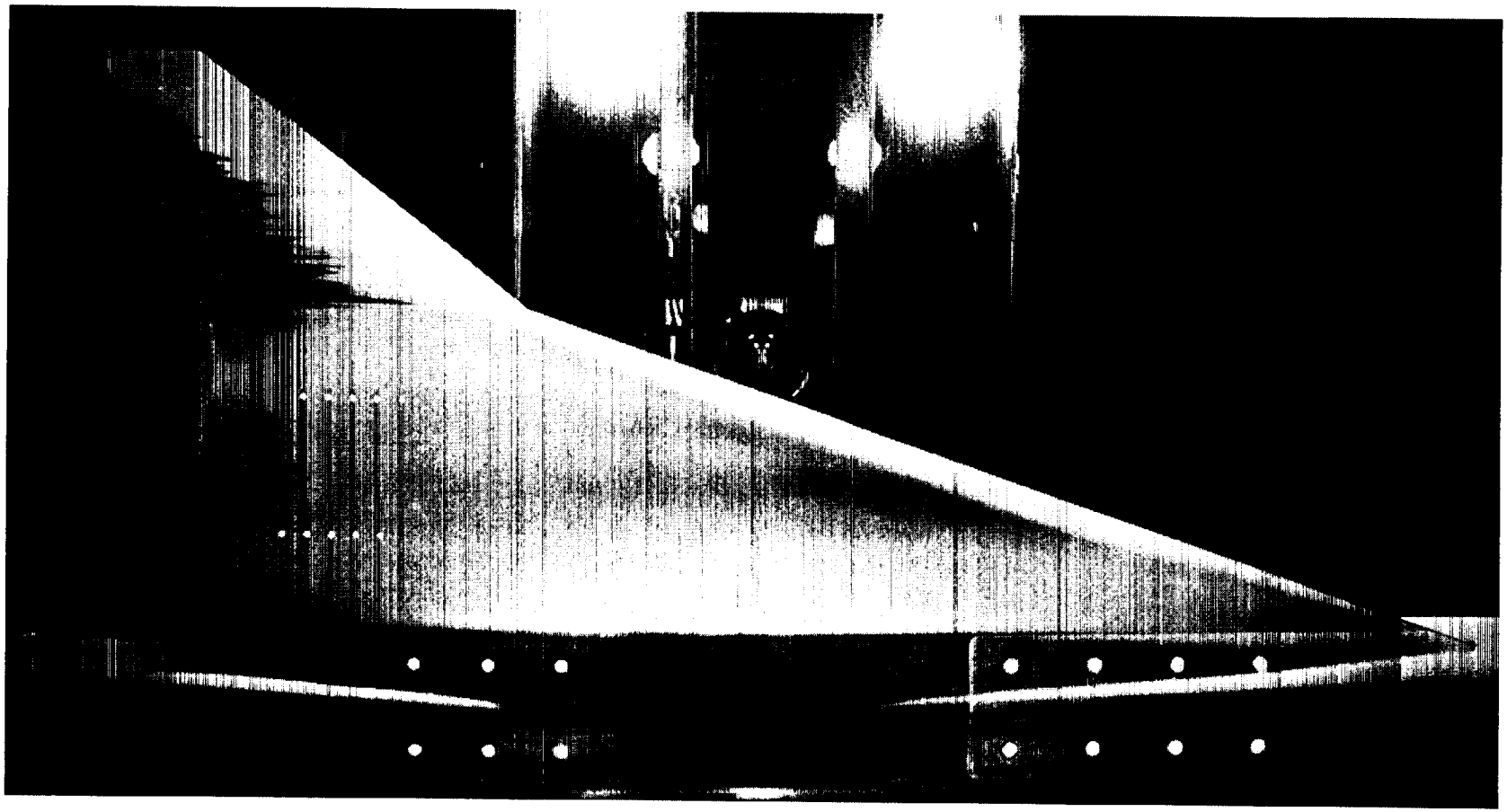

Viewgraph 19: Sublimation Photo, 0.012" Trip Dot, Upper Surface

This sublimation photograph of the wing upper surface with 0.012" trip dots shows that the trip dots are not effective at tripping the flow in the inboard region, but are more effective in the outboard region away from the break in the planform.

Sublimation Photo

0.012" Trip Dot, Upper Surface

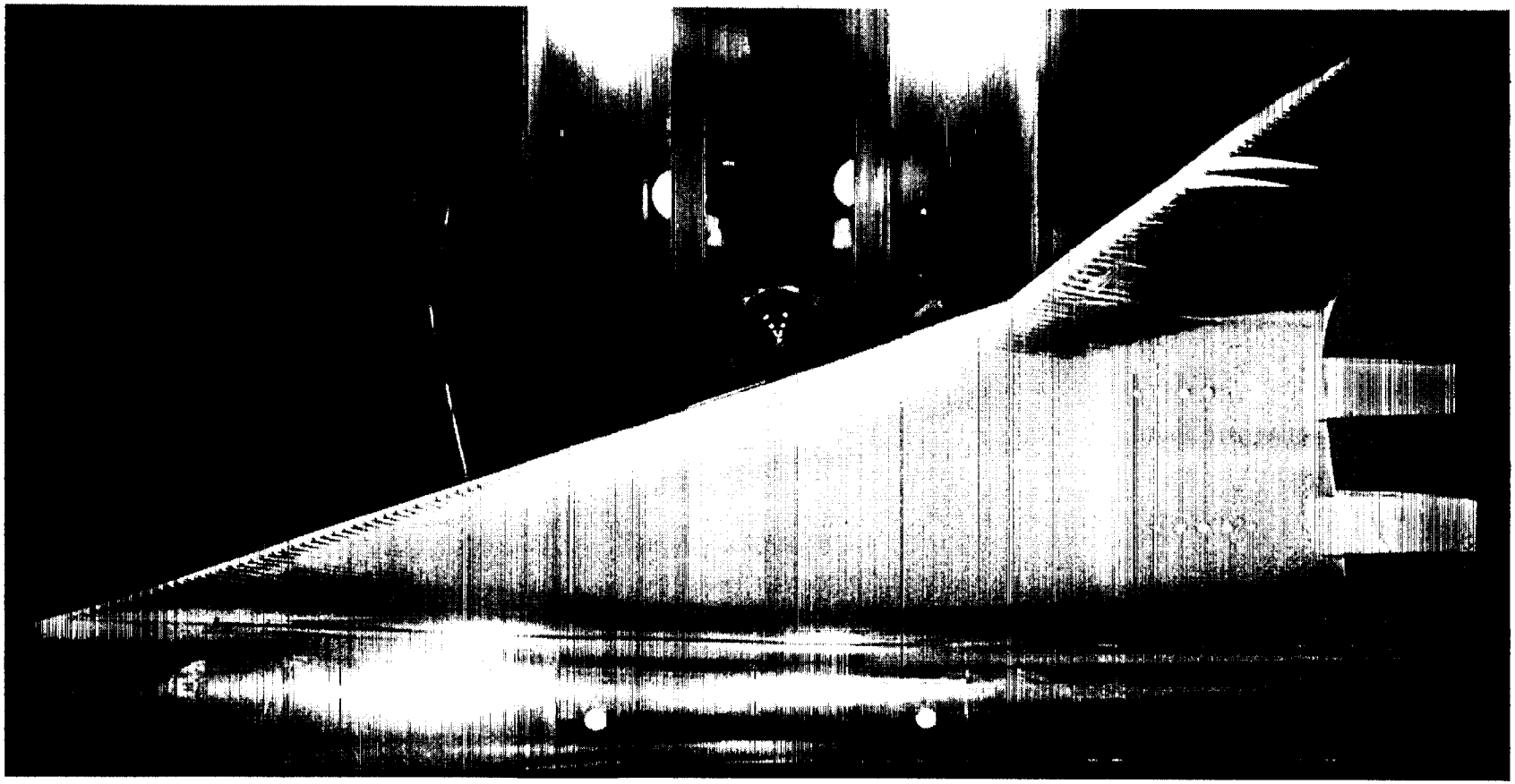

Viewgraph 20: Sublimation Photo, 0.012" Trip Dot, Lower Surface

This sublimation photograph of the lower surface of the wing shows that the 0.012" trip dots are effective at tripping the flow in both inboard and outboard regions. In addition, shock waves produced by the dots are visible in the inboard region.

Sublimation Photo

0.012" Trip Dot, Lower Surface

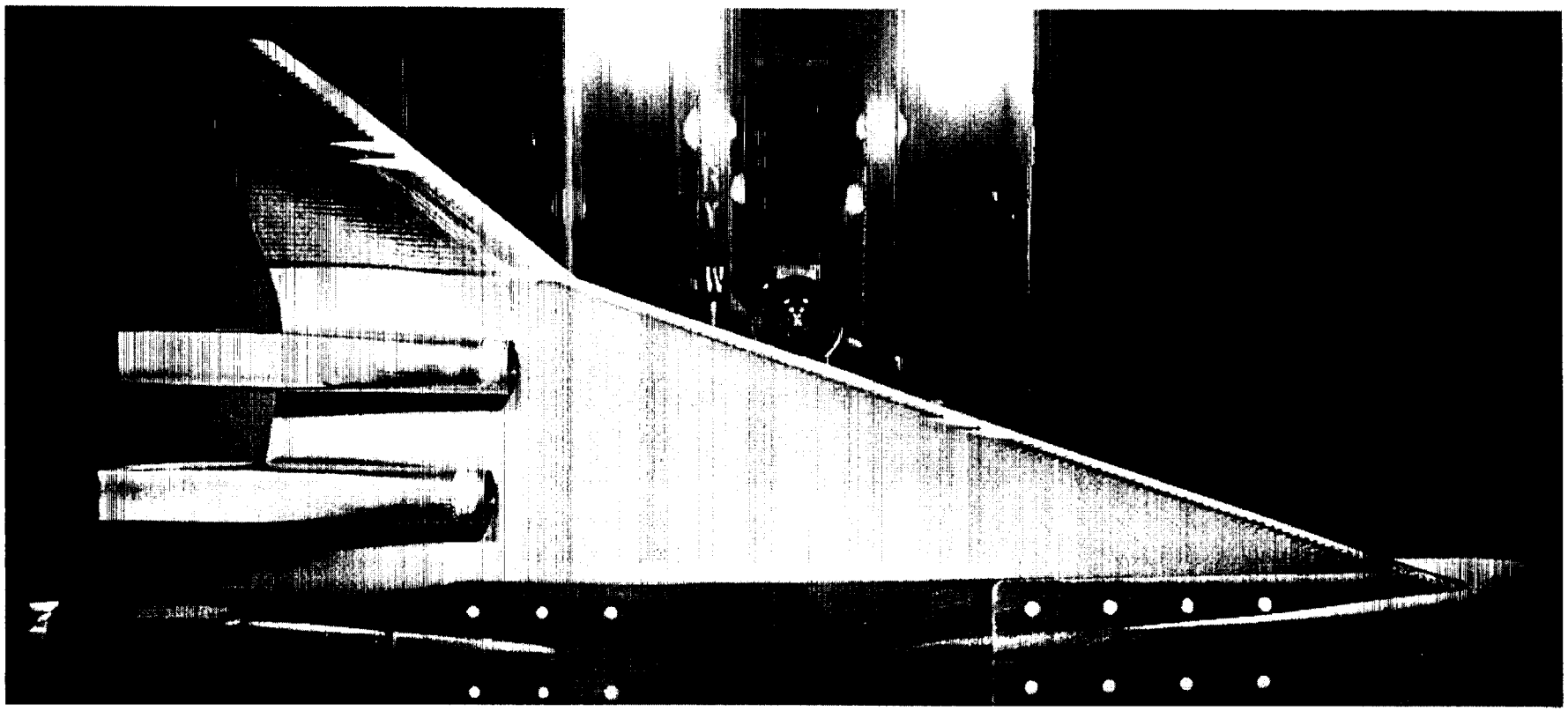

1501

Viewgraph 21: Further Analysis

In order to attempt a meaningful analysis of the variation in drag with trip dot height and possibly estimate the trip drag, the data must be adjusted to reflect the longer laminar run observed on the inboard upper surface. The actual transition location for each trip dot configuration can be measured from the sublimation photographs obtained during the test. Then, a laminar flow correction can be applied to the drag data. Plotting the "corrected" drag data may produce a plateau which would allow a more accurate estimate of the trip drag as a function of trip height.

Further Analysis

- Obtain transition location from sublimation photos
- Apply laminar flow correction for each trip height
- Evaluate resulting drag curve
- Estimate trip dot drag?

This page is intentionally left blank.